Combining Multiple Boundary Shapes in Deformable EIT a Potential Use in Breast Imaging

Jing Hu and Manuchehr Soleimani

Abstract—**A few emerging medical imaging methods are being developed for breast imaging. Electrical impedance tomography (EIT) is an excellent candidate for safe, low cost and non-invasive breast cancer monitoring. Despite early promises, the EIT faces a few challenges for the breast imaging application. It is mainly due to its limited resolution and especially for the tumours in depth. However, unlike the other medical applications of EIT, such as brain and thorax, breast tissues are deformable. This paper exploits the deformation of breast shape to enhance the EIT resolution and its depth detection. Exterior boundary of the breast can be used to create deformable EIT with multiple shapes to enhance the imaging resolution, turning a challenge to an opportunity. With deformation of the boundary shape, more independent measurements can be obtained, and hence more information can be gained. This can increase the resolution of the reconstructed image and possible detection for smaller tumours in depth. This paper demonstrates this by experimental verification in test phantom representing tumour size inclusion deep inside breast by a few deformed shape phantoms. To evaluate the experimental results, 3D printed phantoms are built in several different shapes. Quantitative image analysis shows that some of the deformed shapes are superior to traditional circular cross section. Additionally, we proposed a combination of data from all shapes so that all this information can be used in one step reconstruction to achieve higher imaging accuracy.**

Index Terms—Breast cancer diagnosis, electrical impedance tomography, deformed boundaries in EIT

I. Introduction

Breast cancer is taking many lives in many parts of the world as the leading cause of cancer death in women [11]. Modalities of diagnosis and treatments have been improving the situation over the last decade. Further improvement of diagnostics is still needed. Studies show that early diagnosis of breast cancer is considered vital because of a five-year survival rate of 96% for those whose cancer was detected in the early stages).

Manuscript submitted Feb 02, 2020. J Hu and M. Soleimani are with the Engineering Tomography Laboratory (ETL), Department of Electronic and Electrical Engineering, University of Bath, Claverton Down, BA2 7AY, UK. (e-mail: jh460@bath.ac.uk, m.soleimani@bath.ac.uk.)

Breast imaging by standard film screen mammography takes most of the credit for helping reduce the death rate of the disease. Mammography includes use of X-ray, which has radiation involved [8], and produces false positive, denser breast for younger patient. In addition, alternative breast imaging technologies have undergone developments considerably for analysis, detection, evaluation, and diagnosis. Emerging technologies in breast cancer imaging such as X-ray CT, Ultrasound elastography, Magnetic Resonance Imaging (MRI), and PET are considered [3], [4],[7], [9], [14], [15]. Ultrasound tomography, Microwave tomography and optical imaging are amongst next generation of the new method considered for breast imaging. Patient safety during the imaging, cost of imaging system, and its ease of use is still an inspirational task to reach as wide as possible communities for breast cancer screening. Electrical impedance tomography (EIT) is an imaging technique under investigation for a few clinical applications such as thorax, brain, breast screening [6], [7], [10], [13]. The principle is to reconstruction image of the region of interest by mapping the electrical conductivity distribution of the area. Electrical impedance measurements are used via injection of small electrical current through electrodes attached to the exterior of the object to achieve a safe and low-cost imaging in EIT. Among all the medical imaging technologies, EIT has the advantage of its low cost, mobility and its non-invasive nature. However, it suffers from low spatial resolutions. This paper aims to investigate the feasibility of improvement of EIT application in breast cancer detecting by deformable boundary EIT [1]. This paper extends the idea of [1] by demonstrating it with lab-based experiments. One of the most significant issues about EIT systems is that the resolutions of the reconstructed images are low compared to other conventional medical imaging technologies such as CT, X-ray or MRI. Early detection of the tumours in their primary stage will increase the patient's chance of living significantly. The EIT system has been developed for breast cancer imaging and some systems are developed and tested. Both in vitro and in vivo data have suggested a role EIT application for breast cancer detection. Since early stage tumour means small size anomalies, the low resolution of EIT is a barrier for its safe and regular use. In this paper we aim to demonstrate a multiple shape EIT to enhance its resolution. It is possible to deform breast because of its soft tissue structure. Various deformation models of breast shape are proposed with hope that each deformation could create new and independent EIT measured data enabling more robust and high-resolution imaging. Simulation analysis in [1] shows this is indeed the case, that objects of much smaller size and in depth could be detected by such a combined shape approach. More independent data provides more information from the same region of interest. The hypothesis is: can we show that using combined multiple data from different shapes a higher accuracy and resolution be achieved using experimental testing situation? In this hypothesis, the information gathered with different deformed shapes are combined and they all contribute to information about the anomalies deep inside breast. Phantom studies have been designed and carried out to demonstrate the concept of combined multiple shape EIT idea for potential use in breast cancer imaging. Sets of experiments are carefully designed to validate the results. The focus in here is for tumour in depth as EIT already works well to detect anomalies near to the exterior boundary.

II. Method

In this section we describe the modelling aspect of the multiple shape EIT in terms of forward modelling, inversion of individual shapes and combined shape. All these done in context of limited region of interests for image reconstruction. Forward problem of EIT is solving electric potential with assumed conductivity distribution σ. For most of EIT problems, moderate frequencies would be applied to the conductive region, and in this paper, experiments are on frequencies between 10 kHz to 200 kHz, which could be considered as low frequency EIT. The EIT has three main components of computational software, sensor and data collection system. The computational models involved field electrical modelling for forward model and inversion algorithm to recover conductivities from voltage measurements. EIT systems consist of electrodes on the boundary for driving and measuring purposes. For the appropriate formulation of the system, the complete electrode model (CEM) is used to constrain the boundary conditions. Electrically conductive field model can be used as EIT main equation

$$\nabla \cdot (\sigma \nabla u) = 0 \quad x \in \Omega \quad (1)$$

describes the potential field $\mathbf{u}$ within the boundary, with internal electrical conductivity of $\boldsymbol{\sigma}$ and the voltage measurement at the electrode U_k is described by the complete electrode model

$$U_k = u + Z_k \sigma \frac{\partial u}{\partial \hat{n}} \quad x \in e_k \, ; k = 1,2, \dots, k \quad (2)$$

can be used, where u is the potential field, Z_k is the contact impedance, $\hat{n}$ is the outward unit normal vector and e_k is the electrodes. To be able to image a domain, it is essential to turn the continuous problem into a discrete problem. The finite element method (FEM) is a numerical discretizing method commonly used in EIT, and it discretizes the domain of interest into small elements to solve the forward model [2], [5]. In our case, one of the major challenges is that with deformable boundary, the boundary shapes change for each set of measurements. Therefore, with multiple shapes, multiple forward models are required. At this stage, the selection of shapes is entirely arbitrary. To combine the information, a combined Jacobian matrix is formed, and the equation of the system is as follows

$$\begin{bmatrix} \Delta V_1 \\ \Delta V_2 \\ \vdots \\ \Delta V_5 \end{bmatrix} = [J_1; J_2; \cdots; J_5][(\Delta\sigma)] \quad (3)$$

Where ΔV_1, ΔV_2, ΔV_3, ΔV_4, and ΔV_5 are the voltage difference data for shape 1, 2, 3, 4, and 5, and $\mathbf{J_1}$, $\mathbf{J_2}$, $\mathbf{J_3}$, $\mathbf{J_4}$, and $\mathbf{J_5}$, are the Jacobian values for each shape. A standard Tikhonov regularization scheme is adapted in order to calculate the changes in electrical conductivity [12].

$$\Delta\sigma = (J^T J + \gamma^2 I)^{-1} J^T \Delta v \quad (4)$$

To demonstrate the robustness of the proposed method we developed a region of interest imaging. An inclusion will stay in fix position within all five different shapes. Fig. 1 shows a schematic of region of interest. By keeping a region of interest, we avoided the task of co-registration of position of inclusion(s) in different shapes. The lab experiments involve solid and saline water, which are non-elastic, in real breast tumour and breast tissues are both elastic. In future clinical studies, the position of tumour could move with deformed boundary and for that we need to co-register such a position for all different shapes.

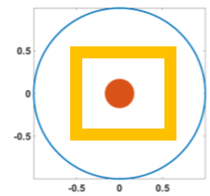

Fig. 1. Region of interest imaging

III. Experimental results

To illustrate the simulation studies in [1], five different shapes of phantoms are made using 3D printer that the reconstruction works for each deformed shape. Electrodes are attached corresponding to the computer model. Location of inclusions for all sets of experiments is marked with the same scale to register the inclusions in the same physical location for different shapes. Fig. 2 is a picture of the phantoms and FEM mesh model we used for tests with marked locations. The length along vertical axis stays the same for all phantom, the same as diameter of circular shape, which has diameter of 10 cm.

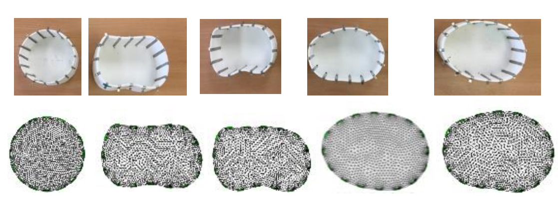

Fig. 2. Five different meshes that are generated for five different shapes

A SwissTom Pioneer (http://www.swisstom.com/) EIT system is used. The Swiss Tom company is now acquired by Sentec AG. We used 16 electrodes (the system can have up to 32 electrodes) is used in 45 kHz excitation frequency and 1mA excitation current. EIT PioneerSet from SwissTom AG is used for the experiments. Interface module connects PC with the Sensor Belt Connector. The system operates at 100-240VAC
50/60KHz and provides injection currents 1-7mA 50kHz-250kHz AC. It is also equipped with programmable injection patterns, and differential/ absolute voltage measurements are taken. The system has high-speed data acquisition of programmable 1-80 data frames per second (SwissTom 2018). Fig. 3 is a block diagram SwissTom system and sensor connection. In experimental studies three inclusions of radiuses of 0.5 cm (inclusion 1), 0.75 cm (inclusion 2) and 1 cm (inclusion 3) are used in single inclusion and multiple inclusions. In this paper the inclusion represent breast tumour and region of interests are deep inside of breast.

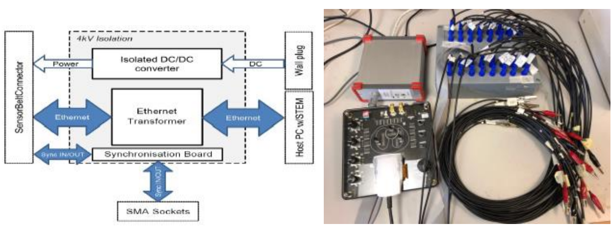

Fig. 3: The block diagram of data collection module and sensor

Figure 4 shows cases (a), (b), (c) and (d) for experimental data collection. Either one or two inclusions are chosen for data collection, data were collected for all 5 shape phantoms of Fig.2 with the inclusion(s) at exact same locations. Quantitative image quality parameters including shape deformation (SD), resolution (RES) and amplitude ration (AR) are selected from widely used GREIT parameters [16].

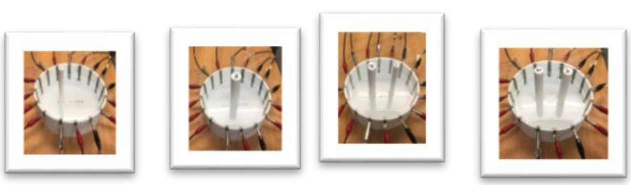

Fig.4 Four experimetal set up, case a small inclusion in left,a large inclusion in centre/left, one large and one small inclusions centre/right, and two large inclusions right

Fig. 5-8 show the reconstruction of inclusion(s) each shape as well as the combined shape approach. In these Figures the top left shows a circular shape with inclusion(s). The same inclusions are used in all five shapes in the same location. Shapes (1), (2), (3), (4), (5) are individual reconstruction from shapes in Fig. 2, and case (6) is combination of all shapes, the reconstructed images are shown in bottom row of Fig. 5-8. Image quality values for RES, AR and SD are shown in plots in top right in Fig. 5-8. In all these cases it is clear from reconstructed images that the combined shape approach produces correct shape of inclusions and their location and the separation between inclusions in case of two inclusions. In reconstructed images, the inclusion (s) are less conductive than the background saline water, blue colour in images are the inclusions. In all these cases for image quality measures are showing high image quality in all parameters using combined shape data (case 6). A traditional circular shape is doing the worth in all cases. RES values, AR and SD values in all these experimental tests shows the case (6) which is combined data from all 5 shapes outperformed all individual shapes. For Fig. 5-8 the image is reconstructed in a region of interest as per Fig. 1. This enables to position the inclusion in the same physical position.

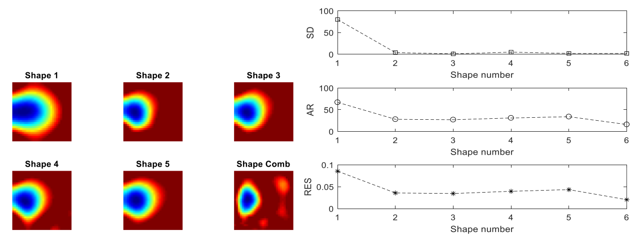

Fig. 5. Reconstruction of single inclusion at top left for case (a), bottom rows reconstruction of shapes 1-5 from Fig. 2, same inclusion in all 5 shapes in the same position, and (6) is when the shapes are combined. Top right shows the image quality measures from five shapes (1-5) and combined shape (6)

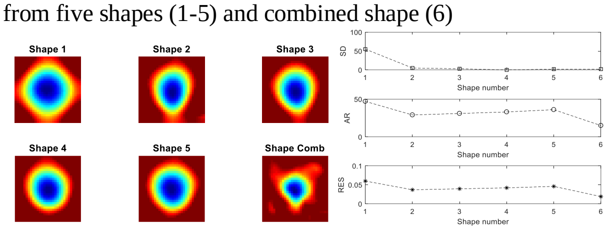

Fig. 6. Reconstruction of single inclusion in center for case (b), bottom rows reconstruction of shapes 1-5 from Fig. 2, and (6) is when the shapes are combined. Top right shows the image quality measures from five shapes (1-5) and combined shape (6)

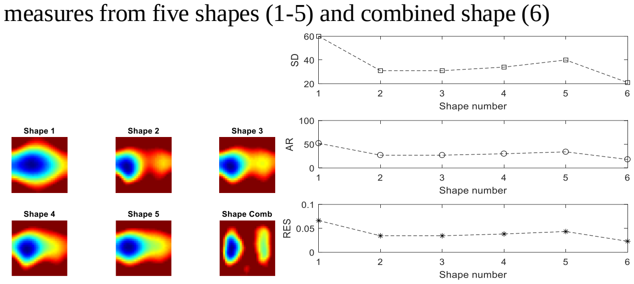

Fig. 7. Reconstruction of two inclusions one large for case (c), one small, bottom rows reconstruction of shapes 1-5 from Fig. 2, and (6) is when the shapes are combined. Top right shows the image quality measures from five shapes (1-5) and combined shape (6)

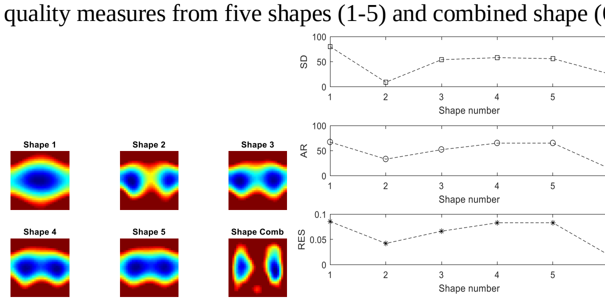

Fig. 8. Reconstruction of two equal size inclusions for case (d), bottom rows reconstruction of shapes 1-5 from Fig. 2, and (6) is when the shapes are all combined. Top right shows the image quality measures from five shapes (1-5) and combined shape (6)

Breast cancer screening and early stage detection of tumour is a critical diagnostic challenge that can help save many lives. Medical imaging is a powerful route for breast cancer detection. Although mammograms are the gold standard for such screening, they use radiation and includes false positive and negative outcome. There is an obvious need for alternative and complementary imaging systems. This study shows a promising approach to enhance EIT for breast imaging. A key limitation of this study is a combination of a liquid background and solid inclusion(s). In real clinical settings, a deformed breast tissue (background) and tumour (inclusion) can move and change its shape and electrical properties. The future study should consider these important elastic-electrical properties when considering deformable EIT. The study focuses on tumours in depth as EIT should work well for tumour close to the exterior boundary.

IV. Conclusions

A deformable EIT is considered for breast imaging in this study. Carefully designed experiments have been carried out to validate the idea of a combined multiple shapes for in depth tumour reconstruction. Phantoms and samples are 3-D printed regarding the simulation model precisely to allow for accurate quantification. By combination of the information gathered for multiple deformations, focusing on region of interests, the reconstructed images have shown much better resolution and accuracy. Both visual and quantitative analysis shows an important improvement of combined EIT data compared to the traditional circular sensor array. All image qualities chosen in this study are showing consistence enhancement and therefore robustness of the proposed combined shape approach. The study also shows a traditional circular shape, which one would choose as a default compliant with the shape of breast cross section indeed has the worth performance. This is particularly true when detection of a tumour in depth is needed. Future studies are needed to account for electromechanical properties of breast tissues under exterior deformation.

References

[1]. Hu, J and M Soleimani, (2017), “Deformable boundary EIT for breast cancer imaging”, Biomedical Physics & Engineering Express. 3, 1, 015004.

[2]. Adler, A and WRB Lionheart, (2006). “Uses and abuses of EIDORS-an extensible software base for EIT”. In: *Physiological Measurement* 27,5, pp. 25– 42.

[3]. Bartella, L and W Huang (2007). “Proton (1H) MR spectroscopy of the breast”. In: *Radiographics*, pp. 241–252.

[4]. Benard, F and E Turcotte (2005). “Imaging breast cancer with single photon computed tomography and positron emission tomography”. In: *Breast Cancer Res*, pp. 153–162.

[5]. Boyle, A, A Adler and WRB Lionheart, (2012). “Shape Deformation in Two-Dimensional Electrical Impedance Tomography”. In: *IEEE Transactions on Medical Imaging*, pp. 2185–2193.

[6]. Cherepenin, V A et al. (2001). “A 3D electrical impedance tomography (EIT) system for breast cancer detection”. In: *Physiological Measurement*, pp. 9–18.

[7]. Hartov, A, T E Kerner, et al. (2001). “Dartmouth’s next generation EIS system: preliminary hardware considerations”. In: *Physiological Measurement*, pp. 25–30.

[8]. Hendrick, RE (2010). “Radiation doses and cancer risks from breast imaging studies”. In: *Radiology*, pp. 246–253.

[9]. Houten, E W Van et al. (2003). “Initial in vivo experience with steady-state subzone-based MR elastography of the human breast”. In: *J.Magn.Res Imaging*, pp. 72–85.

[10]. Mueller J L, D Isaacson, and J C Newell (1999). “A reconstruction algorithm for electrical impedance tomography data collected on rectangular electrode array”. In: *IEEE Transactions on Biomedical Engineering*, pp. 1379–1386.

[11]. Sree, S V et al. (2011). “Breast imaging: A survey”. In: *World Journal of Clinical Oncology*, pp. 171–178.

[12]. Vauhkonen M, Paivi J et al. (1999). “Three-Dimensional Electrical Impedance Tomography Based on the Complete Electrode Model”. In: *IEEE Transactions on Biomedical Engineering*, pp. 1150–1160.

[13]. Wtorek, J, J Stelter, and A Nowakowski (1999). “Impedance mammography 3D phantom studies”. In: *Ann NY Acad Sci*, pp. 520–533.

[14]. Yi, A et al. (2012). “Sonoelastography for 1786 nonpalpable breast masses: diagnostic value in the decision to biopsy”. In: *Eur Radiol*, pp. 1033–1040.

[15]. Zuley, M L et al. (2013). “Digital breast tomosynthesis versus supplemental diagnostic mammographic views for evaluation of noncalcified breast lesions.” In: *Radiology*, pp. 89–95.

[16]. Adler A. *et al.*, "GREIT: a unified approach to 2D linear EIT reconstruction of lung images," *Physiological measurement,* vol. 30, no. 6, p. S35, 2009.